Journal of Organometallic Chemistry, 249 (1983) 303–313
Elsevier Sequoia S.A., Lausanne – Printed in The Netherlands

THE GEOMETRY AND BONDING OF MAGNESOCENE. AN AB-INITIO MO-LCAO INVESTIGATION

K. FAEGRI, Jr., J. ALMLÖF

Department of Chemistry, University of Oslo, Oslo 3 (Norway)

and H.P. LÜTHI

Department of Inorganic Chemistry, University of Zurich, CH-8057 Zurich (Switzerland)

(Received February 4th, 1983)

Summary

High quality Hartree-Fock calculations for magnesocene yield equilibrium molecular geometry, IR and Raman frequencies, and orbital energies. The metal–ring bonding is mainly between Mg $3s$ and $3p$ orbitals and the ring π systems. The somewhat special bonding situation combined with the long metal–ring distance leads to a shift of valence charge towards the ligands, leaving a high local Mg effective charge.

A. Introduction

Recently, a number of investigations have shown ferrocene and related sandwich compounds to present a formidable challenge to ab-initio MO-LCAO calculations at the Hartree-Fock level [1–3]. Even high-quality calculations yield equilibrium metal–ring distances in poor agreement with experimental data, resulting in an error of 0.25 Å for the worst case (ferrocene [2]). Numerous compounds have been investigated, and, although the error in energy-optimized metal–ring distances appears to be a salient feature of these calculations, no explanation of the phenomenon is readily at hand. (A summary and discussion of all these calculations will be published elsewhere.) Most of the calculations have been performed on complexes where the central atom is either a transition metal or a Group IVA metal-elements which readily form this type of compound.

Magnesocene, $Mg(C_5H_5)_2$ (abbreviated as $MgCp_2$), is easily prepared [4], relatively stable, and much used as a starting compound in the synthesis of other cyclopentadienyl compounds, as a host molecule for EPR investigations [5], and even as a catalyst for polymerizations. This species occupies an interesting position at the lighter end of the series of dicyclopentadienyl sandwich compounds and is

0022-328X/83/$03.00

distinguished by the fact that the central atom has no *d*-electrons available for bonding. Thus, the bonding situation is somewhat different from that of the transitions metals, giving rise to a discussion of the type and mechanism of the metal–ring bonding. Considerable disagreement still exists as to whether this compound should be classified as ionic or covalent.

Early investigations of magnesocene were carried out by Weiss and Fischer [6] who found a regular staggered sandwich (D_{5d}) geometry from an X-ray diffraction study. Wilkinson et al. [7] interpreted the regular sandwich structure as primarily a result of electrostatic balances in an entirely ionic system, basing their conclusions on the solubility and conductivity observed in liquid ammonia and on the reactivity in exchange reactions and hydrolysis. The idea of ionic bonding was also advanced in a mass-spectrometric investigation by Friedman et al. [8] on the grounds of the high abundance of $MgCp^+$ ions in contrast to the behaviour of ferrocene, which yields $FeCp_2^+$ as the most abundant ion. From a largely theoretical consideration of overlaps and ionization potentials, Cotton and Reynolds [9] concluded that the transfer of two Mg electrons to the cyclopentadiene rings is energetically favored over the promotion to a $3p^2$ bonding configuration, and that the ionic bond may be stabilized by Mg–Cp e_{1u} overlap and also possibly by back-donation to the Mg $3s$ orbital.

Arguments in favor of a covalent bonding situation were advanced by Lippincott et al. [10] in the first major IR and Raman spectroscopic investigation of magnesocene. The low intensity observed for the asymmetric ring–metal stretch disagrees with that estimated from a zero order effective charge model for an ionic compound, and thus indicates covalent bonding. Also, the similarity of the magnesocene and ferrocene spectra, the solubility of magnesocene in benzene and cyclohexane, and the fact that no qualitative changes were seen in passing from the spectrum of the solid to a spectrum recorded in solution appeared to support this argument. However, in a subsequent study Aleksanyan et al. [11] argue that the perturbations of those parts of the spectra which can be assigned to Cp^- are very slight compared to the strong perturbations observed in covalent sandwich compounds like ferrocene, and this indicates ionic bonding. Finally, Haaland et al. [12] on the basis of semi-empirical (CNDO2) MO calculations argue that the bonding is covalent and mainly between the *p*-orbitals on Mg and the e_{1u} π system on the rings with a charge separation probably not much greater than in ferrocene.

Against this background of conflicting experimental and theoretical evidence, and because of our general interest in calculations on metal-sandwich compounds, we decided to carry out high-quality ab-initio calculations for the magnesocene molecule.

B. Computational details

Rather extensive calculations on ferrocene [2] have shown that the optimized metal–ring distance is quite insensitive to the basis set size and that this structural parameter is conserved at the double zeta level. It is by no means clear, however, that this insensitivity to basis set size is necessarily retained when iron is replaced by an element with rather different chemical properties. We have therefore carried out calculations with several basis sets ranging from a minimal basis to a better than triple zeta plus polarization set. The basis sets used have all been selected from

TABLE 1

BASIS SETS

Primitives	Source	Added functions	Contraction	Mnemonic
Mg:				
10*s* 6*p* 1*d*	Ref. 20	3*s*: $\zeta = 0.45$, 3*s*: $\zeta = 0.07$	3*s* 2*p* 1*d*	RS 32
		3*d*: $\zeta = 0.10$		
			6*s* 4*p* 1*d*	RS 641
12*s* 9*p* 1*d*	Ref. 21	3*d*: $\zeta = 0.10$	7*s* 5*p* 1*d*	MC751
12*s* 9*p* 2*d*	Ref. 21	3*d*: $\zeta = 0.70$, 3*d*′: $\zeta = 0.167$	7*s* 5*p* 2*d*	MC752
			7*s* 6*p* 2*d*	MC762
C:				
7*s* 3*p*	Ref. 20	none	2*s* 1*p*	RS21
		none	4*s* 2*p*	RS42
7*s* 4*p*	Ref. 20	2*p*: $\zeta = 0.07$	4*s* 3*p*	RS43
7*s* 3*p* 1*d*	Ref. 20, 21	3*d*: $\zeta = 0.6$	4*s* 2*p* 1*d*	RS421
		3*d*: $\zeta = 0.3$		RS421′
9*s* 5*p*	Ref. 22		4*s* 2*p*	DU42
9*s* 5*p* 1*d*	Ref. 22	3*d*: $\zeta = 0.6$	4*s* 2*p* 1*d*	DU421
10*s* 6*p* 1*d*	Ref. 23	3*d*: $\zeta = 0.6$	6*s* 4*p* 1*d*	DU641
		3*d*: $\zeta = 0.3$		DU641′
H:				
3*s*	Ref. 24	none	1*s*	VD1
			2*s*	VD2
5*s* 1*p*	Ref. 22	2*p*: $\zeta = 0.80$	3*s* 1*p*	DU31

standard compilations and are listed in Table 1.

We take the electron diffraction structure of magnesocene determined by Haaland et al. [12], as the starting point for our geometry optimization. The C–C and C–H distances were kept at their experimentally determined values of 1.423 Å and 1.116 Å, respectively, in a planar arrangement, D_{5h} geometry was retained, and the metal–ring distance was varied to yield an optimum energy for each basis set. From the energies obtained in this variation the fundamental frequency for the symmetric ring–metal stretch was estimated in a harmonic approximation. For one basis set of double zeta quality (Mg:RS64, C:RS42, H:VD2) we also optimized the C–C and C–H distances at a fixed metal–ring distance of 2.001 Å. The rotational barrier was estimated by performing a calculation in D_{5d} geometry with metal–ring distance optimized for D_{5h}.

All calculations were carried out using the DISCO program [13] which takes full advantage of the molecular symmetry.

C. Results and discussion

Total energies and optimized metal–ring distances from our calculations are presented in Table 2 for a number of different basis sets ranging from a minimal basis to a polarized better than triple zeta set. The largest of these sets, consisting of 337 contracted basis functions, should be close to the Hartree-Fock limit for the properties considered here. Table 2 shows that, in contrast to observations for ferrocene, the calculated metal–ring distance in magnesocene is sensitive to basis set

TABLE 2

TOTAL ENERGIES (E), OPTIMIZED METAL–RING DISTANCE (R(M–R)), DEVIATION OF R(M–R) FROM EXPERIMENTAL VALUE OF 2.008 Å [12] (ΔR(M–R)), AND FUNDAMENTAL VIBRATION FREQUENCY FOR SYMMETRIC STRETCH ($h\omega_0$)

Basis set			E (Hartrees)	R(M–R) (Å)	ΔR(M–R) (Å)	ν_0 (cm^{-1})
Mg	C	H				
RS32	RS21	VD1	−582.7675	2.056	0.048	230
RS641	RS42	VD2	−583.5529	2.079	0.071	224
RS641	RS43	VD2	−583.5665	2.080	0.072	222
RS641	RS421	VD2	−583.7581	2.051	0.043	221
RS641	RS421′	VD2	−583.6913	2.086	0.078	206
MC751	DU42	VD2	−583.9684	2.072	0.064	219
MC752	DU42	VD2	−583.9747	2.058	0.050	223
MC752	DU421	VD2	−584.1366	2.031	0.023	220
MC762	DU641′	DU31	−584.1616	2.033	0.025	216
MC762	DU641	DU31	−584.2160	2.040	0.032	223

size. As the basis set size is increased there is a steady decrease towards the experimental value of 2.008 Å found by Haaland et al. [12]. The minimal basis falls outside the general trend, presumably due to a superposition error. This assumption is supported by the abnormally high value found for the vibrational frequency of the metal–ring symmetric stretch. It is also interesting to note that the use of d-functions in the carbon basis causes significant improvements in the metal–ring distance; regardless of which basis set is used, inclusion of d-orbitals shortens the optimum distance by 0.02 to 0.03 Å. For the largest of these basis sets the error in the calculated metal–ring distance is an order of the magnitude smaller than the corresponding error for ferrocene, indicating that whatever the sources of the large error in ferrocene be, they are either absent or cancel in magnesocene.

The partial geometry optimization performed as described above yields a C–H distance of 1.064 Å and a C–C distance of 1.416 Å compared to the gas electron diffraction (GED) results of 1.116 and 1.423 Å, respectively (see Table 3). The C–C distance is somewhat shorter than experiment, as is usual for Hartree-Fock-optimized bonds at the double zeta level. From a recent basis set study of benzene [14] we do not expect any great changes to this value upon increasing the basis set. The optimized C–H distance is off by approximately 0.05 Å; however, the determination of C–H distances from GED experiments quite frequently yields bonds considerably longer than those obtained from other types of investigations. Thus, we may conclude that structure optimization of the cyclopentadienyl rings using ab-initio Hartree-Fock calculations gives results showing no unexpected deviations from experiment. In Table 3 we have also included geometrical parameters from the X-ray structure determination by Bunder and Weiss [15]. The shorter metal–ring distance found in the crystal as compared with the GED study may be rationalized in terms of crystal packing forces—according to our estimates a compression of the metal–ring distance by 0.024 Å from equilibrium requires only 0.16 kcal/mol. For the C–C distance the calculations give a value quite close to the averages of the two experimental investigations.

TABLE 3

COMPARISON OF CALCULATED STRUCTURAL PARAMETERS WITH EXPERIMENTAL DATA FROM ELECTRON-DIFFRACTION [12] AND X-RAY DIFFRACTION [15] (Å)

	El-diff	X-ray	calculated
C–Mg	2.339(4)	2.304(8)	2.361
C–C	1.423(2)	1.39(2)	1.416
C–H	1.116(7)	1.00(4)	1.064
Mg–ring	2.008(4)	1.977(8)	2.031

The rotational barrier is found to be 31 cal/mol — one order of magnitude smaller than for ferrocene. Again, the D_{5d} geometry found in X-ray structure investigations may be rationalized in terms of crystal forces.

The fundamental vibration frequencies calculated for the symmetric metal–ring stretch $\nu_4(a_{1g})$ are all reasonably close to the Raman result of Aleksanyan et al. [11] at 218 cm^{-1}. Their assignment of this rather weak line differs from that by Lippincott et al. [10] who assign the ν_4 vibration to a stronger line at 191 cm^{-1}. This line was also observed by Aleksanyan et al., but they assigned it to the symmetric ring tilt $\nu_{16}(e_{1g})$, thus obtaining a line reversal from the spectrum of the covalent ferrocene which they take as favouring a different—i.e. ionic—bonding situation in magnesocene.

A problem in the assignment of the IR spectra is the asymmetric ring–metal stretch $\nu_{11}(a_{2u})$. Lippincott et al. [10] assigned this to a line at 526 cm^{-1} by analogy with the ferrocene spectrum, while Aleksanyan et al. [11] and Aleksanyan and Greenwald [16] suggest a possible frequency reversal between this mode and the antisymmetric ring tilt $\nu_{21}(e_{1u})$ giving frequencies of 524 and 461 cm^{-1} for ν_{21} and ν_{11}, respectively. The antisymmetric ring tilt was measured at 440 cm^{-1} by Lippincott et al.

In an attempt to determine the relative positions of these controversial vibrational modes, we have carried out calculations for all four types of distortion, maintaining a metal–ring distance of 2.008 Å. The calculated vibrational frequencies as well as experimental values from a number of investigations are presented in Table 4, and lead to a number of conclusions. First, the good agreement obtained for the ν_4 frequency (symmetric stretch) is probably fortuitous. Normally, Hartree-Fock calculations yield vibrational frequencies somewhat higher than the experimental values; however, our calculations are really appropriate only for gas phase molecules, and the experimental measurements were made with the compound crystalline, molten, or in solution. As the ν_4 distortion is the one mode requiring the largest spatial extension of the molecule, its frequency may well be phase sensitive, as indicated by the blue-shift in going from melt to crystal (Table 4). Thus it is quite probable that the gas phase frequency of this mode is closer to 180–190 cm^{-1}. Secondly, remembering that Hartree-Fock frequencies may be somewhat high, our calculations support the assignment of ν_{11} (asymmetric stretch) to the 440–460 cm^{-1} region by Aleksanyan et al. [11]. However, our calculated frequency for the asymmetric ring tilt ν_{21} conflicts with all experimental assignments, placing this line around 200 cm^{-1} and at approximately the same frequency as the symmetric tilt ν_{16}. The large relative

shift of this line as compared to ferrocene may be rationalized in terms of the much larger ring–ring distance and the weaker bonding of magnesocene. We have demonstrated the effect of a shorter ring–ring distance in magnesocene by calculating the frequency of the asymmetric tilt mode using the ferrocene metal–ring distance (1.65 Å). This experiment shifts the frequency to approximately 400 cm^{-1}, towards the value 492 cm^{-1} suggested for ferrocene. Unfortunately no far-IR spectroscopic investigations of magnesocene are available, and comparison of our calculated ν_{21} frequency with experiment is therefore precluded.

The orbital energies are listed in Table 5, these are taken from the calculation yielding the lowest total energy and are rather insensitive to basis set size. Only a few of the ionization energies have been measured for magnesocene: Evans et al. [17] have recorded the He(I) photoelectron spectrum for the range of 8 to 18 eV, and Bakke et al. [18] have measured the carbon 1*s* energy. Agreement with experiment is seen to be satisfactory within the approximation of Koopmans' theorem for the valence orbitals. For the carbon 1*s* one would expect rather large relaxation energies, and Koopmans' theorem therefore yields ionization energies that are too high. However, the relative values should still be reliable, and we may therefore consider the chemical shift of the carbon 1*s* level from ferrocene. This shift is calculated to be 0.05 eV, consistent with the experimental shift of 0.09 eV reported by Bakke et al. [18].

From the data in Table 5 and comparison with the separated neutral fragments Mg and C_5H_5 it is seen that the orbitals affected by bonding are $5e_1'$, $5a_2''$, and $6a_1'$ —all of which combine Cp π orbitals with Mg 3*s* and 3*p* orbitals. In the neutral Mg atom the 3*s* orbital energy is calculated to be −6.88 eV. In bonding this stabilizes the Cp a_1' π level by almost 2 eV, whereas the Cp levels that interact with Mg 3*p* orbitals are lowered by approximately 1 eV. Thus, our calculated orbital energies support the simple mechanistic picture of Cotton and Reynolds [9] in which the 3*s* electrons are promoted to vacancies in the Mg $3p_{x,y}$–Cp π e_1' combination. However, an essential feature of this model is the concomitant stabilization of the two a_1' Cp orbitals. It might therefore be more appropriate to regard the bonding as taking place through an overall redistribution of electrons within the Cp π–Mg 3*s*,3*p* manifold. We note also that the highest occupied orbital, $4e_1''$, is not shifted from its value in the neutral ring, indicating no participation of Mg *d*-orbitals in the bonding.

TABLE 4

CALCULATED AND MEASURED VIBRATIONAL FREQUENCIES FOR VIBRATIONS ν_4, ν_{11}, ν_{16}, AND ν_{21}. ALL FREQUENCIES IN cm^{-1}

Freq. no.	Calcd.	Melt [a]	Crystal [a]	Soln. [b]	Soln. [c]	KBr [b]	Mode
ν_4 (a_{1g})	224	218	233	191			Symm. metal–ring stretch
ν_{11} (a_{2u})	483		461	526	450	524	Asym. metal–ring stretch
ν_{16} (e_{1g})	230	189	207	229			Symm. ring tilt
ν_{21} (e_{1u})	237		524	440	523	441	Asym. ring tilt.

[a] Ref. 11. [b] Ref. 10. [c] Ref. 16.

TABLE 5

ORBITAL ENERGIES FOR MAGNESOCENE. THE ORBITALS ARE CLASSIFIED ACCORDING TO D_{5h} SYMMETRY. FOR COMPARISON ORBITAL ENERGIES FOR INFINITELY SEPARATED SYSTEMS OF Mg AND C_5H_5 (Mg/Cp) AND Mg^{2+} AND $C_5H_5^-$ (Mg^{2+}/Cp^-) ARE INCLUDED. ALL ENERGIES IN eV

Orb	ε	Character	Mg/Cp	Mg^{2+}/Cp^-	Exp
$4e_1''$	−8.22	Cpπ	−8.16	−0.18	−8.11 [a]
$5e_1'$	−9.09	Cpπ + Mg3$p_{x,y}$	−8.16	−0.18	−9.03 [a]
$3e_2''$	−14.05	C–H	−14.32	−8.03	
$3e_2'$	−14.08		−14.32	−8.03	
$5a_2''$	−14.17	Cpπ + Mg3p_z	−13.22	−7.45	Band from −12.2
$3e_1''$	−14.68	C–H	−14.87	−8.64	to −13.5 [a]
$4e_1'$	−14.70		−14.87	−8.64	
$6a_1'$	−15.09	Cpπ + Mg3s	−13.22	−7.45	
$4a_2''$	−18.80	C–H	−19.00	−12.77	
$5a_1'$	−18.85		−19.00	−12.77	
$2e_2''$	−19.74	C–C σ	−19.96	−13.77	Band from −16.65 [a]
$2e_2'$	−19.79		−19.96	−13.77	
$2e_1''$	−25.84		−25.89	−19.51	
$3e_1'$	−25.89		−25.89	−19.51	
$3a_2''$	−31.66		−31.62	−24.94	
$4a_1'$	−31.75		−31.62	−24.94	
	−62.21	Mg2p	−62.10	−81.82	
	−102.37	Mg2s	−102.5	−122.0	
	−305.64	Cls [c]	−306.2	−299.5	290.12 [b]
	−1334.22	Mg1s	−1334.4	−1354.4	

[a] Ref. 17. [b] Ref. 18. [c] Average of values from 305.62 to 305.67.

We return to a further discussion of orbital energies below when considering the nature of the metal–ligand bond.

Thus, geometry optimization, calculated vibrational frequencies, and orbital energies all indicate that the ab-initio MO − LCAO calculations at the Hartree-Fock level give a satisfactory account of the electronic structure and geometry of magnesocene, in contrast to results for most of the heavier metallocenes, for which calculations fail to reproduce the measured metal–ring distances. As pointed out previously, Mg has no *d*-electrons available for bonding, and the promotion energy for a d^2 configuration is high. In addition the metal–ring distance is rather long, and corresponds to a Mg–C bond at least 0.1 Å longer than what is known from other organomagnesium compounds [15]. Neglect of ring–ring dispersion forces has been cited as one possible source of the failure of Hartree-Fock calculations on ferrocene; these forces are strongly dependent on the metal–ring distance, and it is clear that their importance would be significantly reduced in magnesocene. Similar considerations apply to possible ring-to-metal charge transfer which is another correlation effect that might reduce the metal–ring distance. However, one should keep in mind that the metal–ring distance is even greater in germanocene derivatives, where the error in the calculated distance is 0.11 Å [3]. Finally, we also note that possible relativistic effects would be expected to be much smaller for the light magnesium atom than for transition metals and heavier elements.

The question still remains whether this theoretical electronic structure provides further insight into the nature of the metal–ring bond in magnesocene. Table 5 shows the Mulliken population analysis for four of the basis sets we used. As can be seen, the value for the metal charge fluctuates wildly, and a pure ionic structure is obtained only for the (unrealistic) single zeta basis. One problem here is that the Mulliken population analysis frequently fails to produce meaningful results when the basis set contains diffuse polarization functions (see ref. 2 for a further discussion of this). In this case the 3*d* functions Mg cause of most of these problems; apparently they are used mainly to improve the description of electron distribution on the rings. The problem is further complicated by the fact that the *d*-orbitals used also include the sixth, totally symmetric, combination which serves to improve the *s*-orbital set. On this background one may compare the charges obtained from basis set II in Table 6. (double zeta quality) with results obtained in a similar calculation on ferrocene which yields values of +1.03, −0.36 and +0.26 for Q(Fe), Q(C) and Q(H), respectively. Our magnesocene result disagrees with the estimate of +0.3 for the carbon charge in magnesocene by Bakke et al. [18]. However, as previously mentioned, the chemical shift in the carbon 1*s* binding energies measured by the same authors for magnesocene and ferrocene is quite small, indicating that the shift in carbon charge must be rather modest.

The futility of carrying the Mulliken population analysis beyond the double zeta level is amply demonstrated by our two largest basis sets (IV and V of Table 6). These two sets differ only in the carbon *d*-orbital exponents, yet produce very different Mg populations. If these two calculations really reflected a transfer of charge, one would expect orbital energies to be greatly affected, whereas they show only insignificant variations. Thus one is forced to conclude that as far as the metal

TABLE 6

GROSS ATOMIC CHARGES AND Mg POPULATIONS FOR BASIS SETS OF VARYING SIZE [a]

Basis	I	II	III	IV	V
Gross atomic charges					
Q(Mg)	+2.09	+0.96	+0.72	+0.63	+1.39
Q(C)	−0.41	−0.35	−0.33	−0.22	−0.29
Q(H)	+0.20	+0.26	+0.15	0.15	−0.15
Mg populations					
1*s*	1.998	1.948	1.976	1.975	1.976
2*s*	1.950	2.020	2.004	1.988	1.988
$2p_{xy}$	1.990	1.984	1.985	1.983	1.985
$2p_z$	1.989	1.987	1.991	1.980	1.986
3*s*	0.213	0.489	0.390	0.366	0.219
$3p_{xy}$	0.123	0.219	0.235	0.210	0.174
$3p_z$	−0.015	−0.112	−0.040	0.296	0.169
3*d*	−0.451	0.303	0.520	0.027	0.031
3*d*′				0.357	−0.072

[a] I: (Mg: RS32), (C: RS21), (C: VD1)
II: (Mg: RS641), (C: RS42), (H: VD2)
III: (Mg: RS641), (C: RS421), (H: VD2)
IV: (Mg: MC762), (C: DU641), (H: DU31)
V: (Mg: MC762), (C: DU641′), (H: DU31)

charge is concerned, the Mulliken population analysis is rather unreliable. The Q(C) appear quite stable throughout the various basis sets, and our remarks about the carbon 1s shifts above retain their validity.

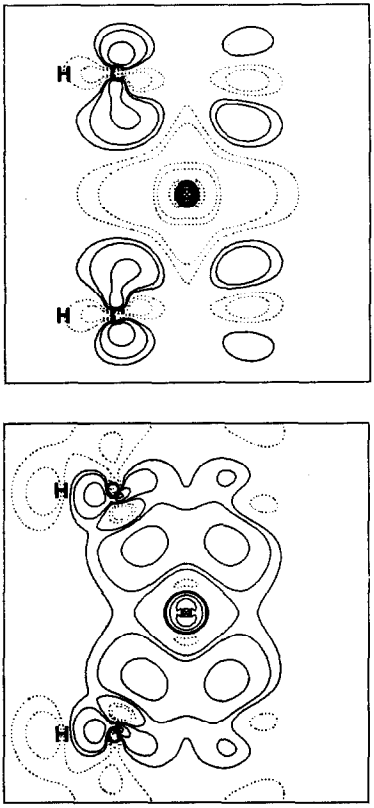

Fig. 1. Density difference plots. Top: Difference between magnesocene and neutral fragments (Mg and Cp). Bottom: Difference between magnesocene and ionic fragments (Mg^{2+} and Cp^{-}). Contours: 0.001, 0.002, 0.005, 0.01, 0.02, 0.05, 0.1.

Further insight may be obtained from plots of the difference in calculated electron density between the neutral metal + cyclopentadiene and magnesocene, and also from the calculated density difference between metal ion + cyclopentadienyls and magnesocene (Fig. 1). The most obvious feature of these plots is the charge transfer from the neutral metal to the rings. However, a pure ionic picture grossly exaggerates this transfer, as shown by the difference plots using ionic fragments. The transferred charge goes mainly into the ring π orbitals, but it is interesting to note that there is also a slight shift of charge from the σ to the π system on the rings during bonding. Perhaps more interesting is the apparent surplus of electrons in the Mg core region of the molecule, this is due to stronger bonding of core electrons as valence electrons are shifted away in the bonding orbitals. It is surprising that even compared to the ionic fragments there is a surplus of Mg core electron density, indicating a contraction of this core region which may be interpreted in terms of a

local effective charge somewhat greater than +2. A calculation of the dipole moment for a 0.03 Å shift of the Mg atom towards one of the rings (asymmetric stretch) yielded a value of 0.296 D, indicating an effective charge of +1.93.

Information about the charge distribution may also be obtained from the orbital energies of Table 5 if we compare the molecular values with those of the neutral (Mg/Cp) and ionic (Mg^{2+}/Cp^{-}) fragments, respectively. It is clear from these data that a pure ionic system, as suggested by Wilkinson et al. [7], would show very large orbital energy shifts, particularly for the non-bonding orbitals. No such shifts are observed, and our calculated orbital energies correlate nicely with those of the neutral systems as well as with measured ionization potentials for valence orbitals. Thus, a shift of approximately 2 electrons away from the core region of Mg accompanied by a contraction of the remaining electron density appears to take place during bonding. In order to effect any bonding, this separation of core and valence density for Mg is quite large, thereby giving rise to the large effective charge observed in the dipole estimate. However, most of the shifted valence density remains within the Mg "sphere of influence", although perhaps only marginally so as evidenced by the large population shifts caused by small changes in carbon *d*-orbital exponents. It is no surprise that the Mulliken population analysis fails under these circumstances.

In conclusion, these calculations display a picture of magnesocene in which the charge separation is slightly larger than that found for ferrocene, though not sufficiently different to justify the classification of one as ionic and the other as covalent. However, at a more subtle level the bonding situation is, indeed, different, as borne out by the fact that the geometry of one of these compounds is essentially correctly described in a high-quality ab-initio calculation whereas the other is not. The metal–ring bond in magnesocene is much weaker than in ferrocene, as indicated by the lower force constant for the metal–ring stretch and by the longer metal–ring distance. This weakness of the bond is due to the fact that bonding is effected in part by promotion of 3*s* electrons to empty 3*p* orbitals which requires considerable energy. Some of the evidence in support of ionic bonding may be rationalized in terms of this weak bond rather than ionicity. This applies to the weakness of the perturbations observed in the Cp^{-} IR and Raman spectra and to the high production rate of $MgCp^{+}$ ions in the mass spectra, as well as the high reactivity observed by Wilkinson et al. [7]. This higher reactivity may be explained by the magnesium atom being more accessible due to the longer metal–ring distance in magnesocene, and by the high apparent effective charge on Mg. Finally, one should note that classification of a sandwich compound as ionic or covalent is of interest mainly in the context of its properties and chemical behavior. Our calculations show that magnesocene represents a complicated bonding situation where classification in terms of such simple concepts is of limited value.

Acknowledgement

The authors thank Drs. A. Haaland, C.J. Nielsen, T.G. Strand, and B.E.R. Schilling for helpful discussions.

References

1 H.P. Lüthi, J. Ammeter, J. Almlöf, and K. Korsell, Chem. Phys. Letters, 69 (1980) 540.
2 H.P. Lüthi, J. Ammeter, J. Almlöf, and K. Faegri, Jr., J. Chem. Phys., 77 (1982) 2002.
3 J. Almlöf, L. Fernholt, K. Faegri, Jr., A. Haaland, B.E.R. Schilling, R. Seip, and K. Taugbøl, Acta Chem. Scand. (1983) in press.
4 W.A. Barber, Inorg. Syn., 6 (1960) 11.
5 J. Ammeter, J. Magn. Reson., 30 (1978) 299.
6 E. Weiss and E.O. Fischer, Z. Anorg. Allg. Chem., 278 (1955) 219.
7 G. Wilkinson, F.A. Cotton, and J.M. Birmingham, J. Inorg. and Nuc. Chem., 2 (1956) 95.
8 L. Friedman, A.P. Irsa, and G. Wilkinson, J. Amer. Chem. Soc., 77 (1955) 3689.
9 F.A. Cotton and L.T. Reynolds, J. Amer. Chem. Soc., 80 (1958) 269.
10 E.R. Lippincott, J. Xavier, and D. Steele, J. Amer. Chem. Soc., 83 (1961) 2262.
11 V.T. Aleksanyan, L.A. Garbuzova, V.V. Gavrilenko, and L.I. Zakharkin, J. Organometal. Chem., 129 (1977) 139.
12 A. Haaland, J. Lusztyk, J. Brunvoll, and K.B. Starowieyski, J. Organometal. Chem., 85 (1975) 279.
13 J. Almlöf, K. Faegri, Jr., and K. Korsell, J. Comp. Chem., 3 (1982) 385.
14 J. Almlöf and K. Faegri, Jr., J. Chem. Phys., (1983) in press.
15 W. Bunder and E. Weiss, J. Organometal. Chem., 92 (1975) 1.
16 V.T. Aleksanyan and I.I. Greenwald, J. Mol. Struc. Theochem, 90 (1982) 35.
17 S. Evans, M.L.H. Green, B. Jewitt, A.F. Orchard, and C.F. Pygall, J. Chem. Soc., Faraday Trans. II, 68 (1972) 1847.
18 A.A. Bakke, W.L. Jolly, and T.F. Schaaf, J. Electron Spectry., 11 (1977) 339.
19 B. Roos and P. Siegbahn, Theoret. Chim. Acta, 17 (1970) 199.
20 A.D. McLean and G.S. Chandler, J. Chem. Phys., 72 (1980) 5639.
21 B. Roos and P. Siegbahn, Theoret. Chim. Acta, 17 (1970) 209.
22 T.H. Dunning, J. Chem. Phys., 53 (1970) 2823.
23 T.H. Dunning, J. Chem. Phys., 55 (1971) 716.
24 F.B. v. Duijneveldt, IBM Research Report, RJ 945, (1971).